

Study of $B \rightarrow \eta' h$

K. Abe,⁹ K. Abe,⁴⁷ I. Adachi,⁹ H. Aihara,⁴⁹ K. Aoki,²³ K. Arinstein,² Y. Asano,⁵⁴
 T. Aso,⁵³ V. Aulchenko,² T. Aushev,¹³ T. Aziz,⁴⁵ S. Bahinipati,⁵ A. M. Bakich,⁴⁴
 V. Balagura,¹³ Y. Ban,³⁶ S. Banerjee,⁴⁵ E. Barberio,²² M. Barbero,⁸ A. Bay,¹⁹ I. Bedny,²
 U. Bitenc,¹⁴ I. Bizjak,¹⁴ S. Blyth,²⁵ A. Bondar,² A. Bozek,²⁹ M. Bračko,^{9, 21, 14}
 J. Brodzicka,²⁹ T. E. Browder,⁸ M.-C. Chang,⁴⁸ P. Chang,²⁸ Y. Chao,²⁸ A. Chen,²⁵
 K.-F. Chen,²⁸ W. T. Chen,²⁵ B. G. Cheon,⁴ C.-C. Chiang,²⁸ R. Chistov,¹³ S.-K. Choi,⁷
 Y. Choi,⁴³ Y. K. Choi,⁴³ A. Chuvikov,³⁷ S. Cole,⁴⁴ J. Dalseno,²² M. Danilov,¹³ M. Dash,⁵⁶
 L. Y. Dong,¹¹ R. Dowd,²² J. Dragic,⁹ A. Drutskoy,⁵ S. Eidelman,² Y. Enari,²³ D. Epifanov,²
 F. Fang,⁸ S. Fratina,¹⁴ H. Fujii,⁹ N. Gabyshev,² A. Garmash,³⁷ T. Gershon,⁹ A. Go,²⁵
 G. Gokhroo,⁴⁵ P. Goldenzweig,⁵ B. Golob,^{20, 14} A. Gorišek,¹⁴ M. Grosse Perdekamp,³⁸
 H. Guler,⁸ R. Guo,²⁶ J. Haba,⁹ K. Hara,⁹ T. Hara,³⁴ Y. Hasegawa,⁴² N. C. Hastings,⁴⁹
 K. Hasuko,³⁸ K. Hayasaka,²³ H. Hayashii,²⁴ M. Hazumi,⁹ T. Higuchi,⁹ L. Hinz,¹⁹ T. Hojo,³⁴
 T. Hokuue,²³ Y. Hoshi,⁴⁷ K. Hoshina,⁵² S. Hou,²⁵ W.-S. Hou,²⁸ Y. B. Hsiung,²⁸
 Y. Igarashi,⁹ T. Iijima,²³ K. Ikado,²³ A. Imoto,²⁴ K. Inami,²³ A. Ishikawa,⁹ H. Ishino,⁵⁰
 K. Itoh,⁴⁹ R. Itoh,⁹ M. Iwasaki,⁴⁹ Y. Iwasaki,⁹ C. Jacoby,¹⁹ C.-M. Jen,²⁸ R. Kagan,¹³
 H. Kakuno,⁴⁹ J. H. Kang,⁵⁷ J. S. Kang,¹⁶ P. Kapusta,²⁹ S. U. Kataoka,²⁴ N. Katayama,⁹
 H. Kawai,³ N. Kawamura,¹ T. Kawasaki,³¹ S. Kazi,⁵ N. Kent,⁸ H. R. Khan,⁵⁰
 A. Kibayashi,⁵⁰ H. Kichimi,⁹ H. J. Kim,¹⁸ H. O. Kim,⁴³ J. H. Kim,⁴³ S. K. Kim,⁴¹
 S. M. Kim,⁴³ T. H. Kim,⁵⁷ K. Kinoshita,⁵ N. Kishimoto,²³ S. Korpar,^{21, 14} Y. Kozakai,²³
 P. Krizán,^{20, 14} P. Krokovny,⁹ T. Kubota,²³ R. Kulasiri,⁵ C. C. Kuo,²⁵ H. Kurashiro,⁵⁰
 E. Kurihara,³ A. Kusaka,⁴⁹ A. Kuzmin,² Y.-J. Kwon,⁵⁷ J. S. Lange,⁶ G. Leder,¹²
 S. E. Lee,⁴¹ Y.-J. Lee,²⁸ T. Lesiak,²⁹ J. Li,⁴⁰ A. Limosani,⁹ S.-W. Lin,²⁸ D. Liventsev,¹³
 J. MacNaughton,¹² G. Majumder,⁴⁵ F. Mandl,¹² D. Marlow,³⁷ H. Matsumoto,³¹
 T. Matsumoto,⁵¹ A. Matyja,²⁹ Y. Mikami,⁴⁸ W. Mitaroff,¹² K. Miyabayashi,²⁴ H. Miyake,³⁴
 H. Miyata,³¹ Y. Miyazaki,²³ R. Mizuk,¹³ D. Mohapatra,⁵⁶ G. R. Moloney,²² T. Mori,⁵⁰
 A. Murakami,³⁹ T. Nagamine,⁴⁸ Y. Nagasaka,¹⁰ T. Nakagawa,⁵¹ I. Nakamura,⁹
 E. Nakano,³³ M. Nakao,⁹ H. Nakazawa,⁹ Z. Natkaniec,²⁹ K. Neichi,⁴⁷ S. Nishida,⁹
 O. Nitoh,⁵² S. Noguchi,²⁴ T. Nozaki,⁹ A. Ogawa,³⁸ S. Ogawa,⁴⁶ T. Ohshima,²³ T. Okabe,²³
 S. Okuno,¹⁵ S. L. Olsen,⁸ Y. Onuki,³¹ W. Ostrowicz,²⁹ H. Ozaki,⁹ P. Pakhlov,¹³ H. Palka,²⁹
 C. W. Park,⁴³ H. Park,¹⁸ K. S. Park,⁴³ N. Parslow,⁴⁴ L. S. Peak,⁴⁴ M. Pernicka,¹²
 R. Pestotnik,¹⁴ M. Peters,⁸ L. E. Piilonen,⁵⁶ A. Poluektov,² F. J. Ronga,⁹ N. Root,²
 M. Rozanska,²⁹ H. Sahoo,⁸ M. Saigo,⁴⁸ S. Saitoh,⁹ Y. Sakai,⁹ H. Sakamoto,¹⁷
 H. Sakaue,³³ T. R. Sarangi,⁹ M. Satapathy,⁵⁵ N. Sato,²³ N. Satoyama,⁴² T. Schietinger,¹⁹
 O. Schneider,¹⁹ P. Schönmeier,⁴⁸ J. Schümann,²⁸ C. Schwanda,¹² A. J. Schwartz,⁵
 T. Seki,⁵¹ K. Senyo,²³ R. Seuster,⁸ M. E. Sevier,²² T. Shibata,³¹ H. Shibuya,⁴⁶
 J.-G. Shiu,²⁸ B. Shwartz,² V. Sidorov,² J. B. Singh,³⁵ A. Somov,⁵ N. Soni,³⁵ R. Stamen,⁹
 S. Stanič,³² M. Starič,¹⁴ A. Sugiyama,³⁹ K. Sumisawa,⁹ T. Sumiyoshi,⁵¹ S. Suzuki,³⁹
 S. Y. Suzuki,⁹ O. Tajima,⁹ N. Takada,⁴² F. Takasaki,⁹ K. Tamai,⁹ N. Tamura,³¹
 K. Tanabe,⁴⁹ M. Tanaka,⁹ G. N. Taylor,²² Y. Teramoto,³³ X. C. Tian,³⁶ K. Trabelsi,⁸
 Y. F. Tse,²² T. Tsuboyama,⁹ T. Tsukamoto,⁹ K. Uchida,⁸ Y. Uchida,⁹ S. Uehara,⁹

T. Uglov,¹³ K. Ueno,²⁸ Y. Unno,⁹ S. Uno,⁹ P. Urquijo,²² Y. Ushiroda,⁹ G. Varner,⁸
 K. E. Varvell,⁴⁴ S. Villa,¹⁹ C. C. Wang,²⁸ C. H. Wang,²⁷ M.-Z. Wang,²⁸ M. Watanabe,³¹
 Y. Watanabe,⁵⁰ L. Widhalm,¹² C.-H. Wu,²⁸ Q. L. Xie,¹¹ B. D. Yabsley,⁵⁶ A. Yamaguchi,⁴⁸
 H. Yamamoto,⁴⁸ S. Yamamoto,⁵¹ Y. Yamashita,³⁰ M. Yamauchi,⁹ Heyoung Yang,⁴¹
 J. Ying,³⁶ S. Yoshino,²³ Y. Yuan,¹¹ Y. Yusa,⁴⁸ H. Yuta,¹ S. L. Zang,¹¹ C. C. Zhang,¹¹
 J. Zhang,⁹ L. M. Zhang,⁴⁰ Z. P. Zhang,⁴⁰ V. Zhilich,² T. Ziegler,³⁷ and D. Zürcher¹⁹

(The Belle Collaboration)

¹*Aomori University, Aomori*

²*Budker Institute of Nuclear Physics, Novosibirsk*

³*Chiba University, Chiba*

⁴*Chonnam National University, Kwangju*

⁵*University of Cincinnati, Cincinnati, Ohio 45221*

⁶*University of Frankfurt, Frankfurt*

⁷*Gyeongsang National University, Chinju*

⁸*University of Hawaii, Honolulu, Hawaii 96822*

⁹*High Energy Accelerator Research Organization (KEK), Tsukuba*

¹⁰*Hiroshima Institute of Technology, Hiroshima*

¹¹*Institute of High Energy Physics,*

Chinese Academy of Sciences, Beijing

¹²*Institute of High Energy Physics, Vienna*

¹³*Institute for Theoretical and Experimental Physics, Moscow*

¹⁴*J. Stefan Institute, Ljubljana*

¹⁵*Kanagawa University, Yokohama*

¹⁶*Korea University, Seoul*

¹⁷*Kyoto University, Kyoto*

¹⁸*Kyungpook National University, Taegu*

¹⁹*Swiss Federal Institute of Technology of Lausanne, EPFL, Lausanne*

²⁰*University of Ljubljana, Ljubljana*

²¹*University of Maribor, Maribor*

²²*University of Melbourne, Victoria*

²³*Nagoya University, Nagoya*

²⁴*Nara Women's University, Nara*

²⁵*National Central University, Chung-li*

²⁶*National Kaohsiung Normal University, Kaohsiung*

²⁷*National United University, Miao Li*

²⁸*Department of Physics, National Taiwan University, Taipei*

²⁹*H. Niewodniczanski Institute of Nuclear Physics, Krakow*

³⁰*Nippon Dental University, Niigata*

³¹*Niigata University, Niigata*

³²*Nova Gorica Polytechnic, Nova Gorica*

³³*Osaka City University, Osaka*

³⁴*Osaka University, Osaka*

³⁵*Panjab University, Chandigarh*

³⁶*Peking University, Beijing*

³⁷*Princeton University, Princeton, New Jersey 08544*

³⁸*RIKEN BNL Research Center, Upton, New York 11973*

- ³⁹*Saga University, Saga*
⁴⁰*University of Science and Technology of China, Hefei*
⁴¹*Seoul National University, Seoul*
⁴²*Shinshu University, Nagano*
⁴³*Sungkyunkwan University, Suwon*
⁴⁴*University of Sydney, Sydney NSW*
⁴⁵*Tata Institute of Fundamental Research, Bombay*
⁴⁶*Toho University, Funabashi*
⁴⁷*Tohoku Gakuin University, Tagajo*
⁴⁸*Tohoku University, Sendai*
⁴⁹*Department of Physics, University of Tokyo, Tokyo*
⁵⁰*Tokyo Institute of Technology, Tokyo*
⁵¹*Tokyo Metropolitan University, Tokyo*
⁵²*Tokyo University of Agriculture and Technology, Tokyo*
⁵³*Toyama National College of Maritime Technology, Toyama*
⁵⁴*University of Tsukuba, Tsukuba*
⁵⁵*Utkal University, Bhubaneswer*
⁵⁶*Virginia Polytechnic Institute and State University, Blacksburg, Virginia 24061*
⁵⁷*Yonsei University, Seoul*

Abstract

We report improved measurements of exclusive two-body charmless hadronic B meson decays $B \rightarrow \eta' h$, where h is a charged kaon or pion or a K^0 . These results are obtained from a data sample that contains 386 million $B\bar{B}$ pairs collected at the $\Upsilon(4S)$ resonance, with the Belle detector at the KEKB asymmetric energy e^+e^- collider. We measure $\mathcal{B}(B^0 \rightarrow \eta' K^0) = (56.6_{-3.5}^{+3.6} \pm 3.3) \times 10^{-6}$, $\mathcal{B}(B^+ \rightarrow \eta' K^+) = (68.6 \pm 2.1 \pm 3.6) \times 10^{-6}$ and $\mathcal{B}(B^+ \rightarrow \eta' \pi^+) = (1.73_{-0.63}^{+0.69} \pm 0.12) \times 10^{-6}$, where the first and second errors are statistic and systematic, respectively. The CP asymmetries in the charged modes are measured and no evidence for direct CP violation is found. We measure $A_{CP}(B^\pm \rightarrow \eta' K^\pm) = 0.03 \pm 0.03 \pm 0.02$ and $A_{CP}(B^\pm \rightarrow \eta' \pi^\pm) = 0.15_{-0.38}^{+0.39} {}_{-0.06}^{+0.02}$.

PACS numbers:

The properties of the decay $B \rightarrow \eta' X_s$ are still to be understood by theory. The channel $B \rightarrow \eta' K$ has the largest branching fraction of all charmless hadronic B decay modes. In the Standard Model (SM) the decay $B \rightarrow \eta' K$ is thought to proceed dominantly via gluonic penguin processes [1, 2, 3]. The diagrams [4] that contribute are shown in Fig. 1. The measured branching fractions for $B \rightarrow \eta' K$ [5, 6, 7] are larger than expectations from the generalized factorization approach [8, 9, 10, 11]. This has led to speculations that SU(3)-singlet couplings unique to the η' meson or new physics [16, 17, 18, 19] contribute to the amplitude.

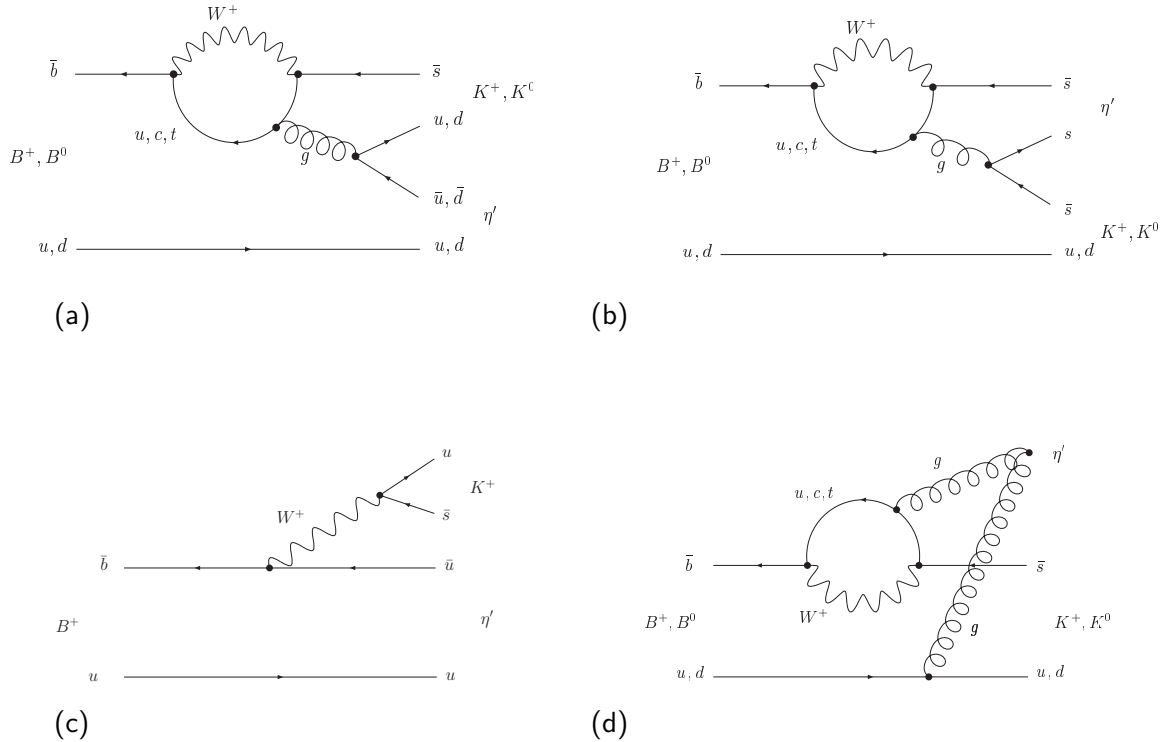


FIG. 1: Feynman diagrams describing the decays $B \rightarrow \eta' K^{+ / 0}$: (a), (b) internal penguins, (c) external tree, (d) flavour-singlet penguin.

The $B^+ \rightarrow \eta' \pi^+$ decay proceeds via similar processes as $B \rightarrow \eta' K$ with $b \rightarrow u(d)$ tree or penguin decays. However, for the latter all contributions are additive, while for the former tree and penguin contributions interfere destructively.

In the SM, direct CP violation arises from the interference of two or more amplitudes with different strong and weak phases [20]. Many charmless hadronic B meson decays contain both tree and penguin amplitudes and provide a rich sample for direct CP violation studies. The decay $B \rightarrow \eta' \pi$ is expected to have comparable contributions from both tree and penguin diagrams, and therefore may have a large asymmetry. For the decay processes dominated by one single amplitude in the SM, a non-zero CP asymmetry may indicate additional amplitudes in the decay and hence provide a hint of new physics. This is also the case for $B \rightarrow \eta' K$, which is thought to proceed entirely through the penguin amplitude and no CP asymmetry is expected.

With the convention that a \bar{B} meson contains a b quark, the direct CP asymmetry in a $B \rightarrow f$ decay is defined as

$$A_{CP} = \frac{\Gamma(\bar{B} \rightarrow \bar{f}) - \Gamma(B \rightarrow f)}{\Gamma(\bar{B} \rightarrow \bar{f}) + \Gamma(B \rightarrow f)},$$

where f is the final state and \bar{f} its CP conjugate. In the experiment we measure the branching fraction $\mathcal{B}(B \rightarrow f)$ and $\mathcal{B}(\bar{B} \rightarrow \bar{f})$, which are proportional to the partial widths.

In this paper, we update the measurements of $B \rightarrow \eta' K^+, \eta' K^0, \eta' \pi^+$ with a sample 35 times larger than our previous dataset [6]. We also report the charge asymmetry of self-tagged decays. All results are based on a data sample that contains 386 million $B\bar{B}$ pairs collected with the Belle detector at the KEKB asymmetric-energy e^+e^- (3.5 on 8 GeV) collider [21]. KEKB operates at the $\Upsilon(4S)$ resonance ($\sqrt{s} = 10.58$ GeV) with a peak luminosity that exceeds $1.5 \times 10^{34} \text{ cm}^{-2}\text{s}^{-1}$.

The Belle detector is a large-solid-angle magnetic spectrometer that consists of a silicon vertex detector (SVD), a 50-layer central drift chamber (CDC), an array of aerogel threshold Čerenkov counters (ACC), a barrel-like arrangement of time-of-flight scintillation counters (TOF), and an electromagnetic calorimeter (ECL) comprised of CsI(Tl) crystals located inside a super-conducting solenoid coil that provides a 1.5 T magnetic field. An iron flux-return located outside of the coil is instrumented to detect K_L^0 mesons and to identify muons (KLM). The detector is described in detail elsewhere [22]. Two inner detector configurations were used. A 2.0 cm beampipe and a 3-layer silicon vertex detector was used for the first sample of 152 million $B\bar{B}$ pairs (Set I), while a 1.5 cm beampipe, a 4-layer silicon detector and a small-cell inner drift chamber were used to record the remaining 234 million $B\bar{B}$ pairs (Set II) [23].

The η' mesons are reconstructed via either $\eta' \rightarrow \eta\pi^+\pi^-$, with $\eta \rightarrow \gamma\gamma$, or $\eta' \rightarrow \rho^0\gamma$. K^0 mesons are reconstructed only via $K_S^0 \rightarrow \pi^+\pi^-$.

Primary charged tracks were selected with $dr < 0.5$ cm and $|dz| < 2.0$ cm, where dr and dz are the impact parameters perpendicular to and along the beam axis, with respect to the run dependent interaction point (IP).

Likelihoods for kaon and pion hypotheses, \mathcal{L}_K and \mathcal{L}_π , are obtained by combining information from the CDC (dE/dx), ACC and TOF systems. The likelihood ratio $\mathcal{R}_K = \mathcal{L}_K/(\mathcal{L}_\pi + \mathcal{L}_K)$ ranges between 0 (pion-like) and 1 (kaon-like) and we require $\mathcal{R}_K > 0.6$ for kaons and $\mathcal{R}_K < 0.4$ for pions from K_S^0 , which keeps about 86% of the kaon/pion candidates, and $\mathcal{R}_K < 0.9$ for pion candidates from the η' decay with an efficiency of about 98%. Prompt pions in $B^+ \rightarrow \eta'\pi^+$ are required to pass the tight selection, $\mathcal{R}_K < 0.1$, which has an efficiency of about 85% and a kaon fake rate of about 4%.

The η meson is reconstructed from two photons, each with an energy of at least 50 MeV. The η mass window is chosen to be $0.5 \text{ GeV}/c^2 < M(\gamma\gamma) < 0.57 \text{ GeV}/c^2$, which corresponds to $+2/-3$ standard deviations (σ) from the nominal η mass given by Particle Data Group (PDG) [24].

We retain ρ^0 candidates in the mass range $550 \text{ MeV}/c^2 < M(\pi^+\pi^-) < 870 \text{ MeV}/c^2$, where $M(\pi^+\pi^-)$ is the ρ^0 candidate mass. We require the transverse momenta of the daughter pions to satisfy the requirement, $P_T(\pi) > 0.2 \text{ GeV}/c$. This suppresses around 40% of background while retaining 86% of the signal.

The requirements for the η' candidate mass depend on the decay channel. For $B \rightarrow \eta'K$ decays, we select η' candidates within $\pm 3.4\sigma$ window for $\eta' \rightarrow \eta\pi^+\pi^-$ ($0.945 \text{ GeV}/c^2 < M(\eta\pi\pi) < 0.97 \text{ GeV}/c^2$) and $\pm 3\sigma$ for $\eta' \rightarrow \rho^0\gamma$ ($0.935 \text{ GeV}/c^2 < M(\rho\gamma) < 0.975$

GeV/c²). For $B^+ \rightarrow \eta'\pi^+$ decay, the η' mass windows are tightened to $\pm 2.5\sigma$ ($0.95 \text{ GeV}/c^2 < M(\eta\pi\pi) < 0.965 \text{ GeV}/c^2$ and $0.941 \text{ GeV}/c^2 < M(\rho\gamma) < 0.97 \text{ GeV}/c^2$). A weak requirement on the η meson decay angular distribution, $h(\eta) < 0.97$, has been applied for the $\eta' \rightarrow \eta\pi^+\pi^-$ mode to suppress combinatorial background, where $h(\eta)$ is the cosine of the angle between the η' momentum and the direction of one of the decay photons in the η rest frame.

K_S^0 candidates are reconstructed from a pair of oppositely charged particles with invariant mass within the range $485 \text{ MeV}/c^2 < M(\pi^+\pi^-) < 510 \text{ MeV}/c^2$. We require the vertex of a K_S^0 to be well reconstructed and displaced from the interaction point and the K_S^0 momentum direction to be consistent with the K_S^0 flight direction.

B meson candidates are then reconstructed combining an η' meson and one of the h candidates. Two kinematic variables are used to extract the B meson signal: the energy difference $\Delta E = E_B - E_{\text{beam}}$ and the beam-energy constrained mass $M_{\text{bc}} = \sqrt{E_{\text{beam}}^2 - P_B^2}$, where E_{beam} is the beam energy and E_B and P_B are the reconstructed energy and momentum of the B candidate in the $\Upsilon(4S)$ rest frame. The events that satisfy the requirements, $M_{\text{bc}} > 5.2 \text{ GeV}/c^2$ and $|\Delta E| < 0.25 \text{ GeV}$ are selected for further analysis.

For events with multiple B candidates, the best candidate is selected based on the χ^2 of a vertex fit, that optimizes a vertex for all charged tracks in the final state, and a mass χ^2 . The latter term is necessary because of the photons in the η' , which may introduce additional multiple candidates even for the same set of charged particles. The formula used to calculate the χ^2 is:

$$\chi^2 = \chi_{\text{vertex}}^2 + [(M(\eta') - m_{\eta'})/\sigma_{\eta'}]^2, \quad (1)$$

with χ_{vertex}^2 being the χ^2 from the charged particle vertex fit, $M(\eta')$ the η' candidate mass and $m_{\eta'}$ the nominal mass of the η' and $\sigma_{\eta'} = 0.008 \text{ GeV}/c^2$ the width of the η' mass distribution. About 10% of events have multiple candidates and of these 10% are due to multiple photons.

Several event shape variables (defined in the center of mass frame) are used to distinguish the more spherical $B\bar{B}$ topology from the jet-like $q\bar{q}$ continuum events. The thrust angle θ_T is defined as the angle between η' momentum direction and the thrust axis formed by all tracks not from the same B meson. Jet-like events tend to peak near $|\cos\theta_T| = 1$, while spherical events have a flat distribution. The requirement $|\cos\theta_T| < 0.9$ is applied prior to any other event topology selections.

Additional continuum suppression is obtained by using modified Fox-Wolfram moments [25] and the angle θ_B between the flight direction of the reconstructed \bar{B}^0 candidate and the beam axis. A Fisher discriminant (\mathcal{F}) [26] is formed by a linear combination of $\cos\theta_T$, S_{\perp} and five modified Fox-Wolfram moments. S_{\perp} is the ratio of the scalar sum of the transverse momenta of all tracks outside a 45° cone around the η' direction to the scalar sum of their total momenta. Probability density functions (PDFs) are obtained from signal and background MC data samples. These variables are then combined to form an event topology likelihood function $\mathcal{L}_c = P_c(\cos\theta_B) \cdot P_c(\mathcal{F})$, where $P_c = \text{PDF}$ of signal (s) or continuum background ($q\bar{q}$). Signal follows a $1 - \cos^2\theta_B$ distribution while continuum background is uniformly distributed in $\cos\theta_B$. We select signal-like events by requiring a likelihood ratio $\mathcal{R}_{\mathcal{L}} = \mathcal{L}_s/(\mathcal{L}_s + \mathcal{L}_{q\bar{q}})$ criteria optimized by MC studies to suppress continuum background. For channels with an $\eta' \rightarrow \rho^0\gamma$ decay an additional variable $\cos\theta_{\mathcal{H}}$, which is the angle between the η' momentum and the direction of one of the decay pions in the ρ rest frame, is included for better signal-background separation.

Further background discrimination is provided by the quality of the B flavor tagging of the accompanying B meson. We use the standard Belle B tagging package [27], which gives the B flavor and a tagging quality r ranging from zero for no flavor and unity for unambiguous flavor assignment. We divide the data into three r regions and separately optimize the \mathcal{R}_L requirements using signal and continuum background Monte Carlo samples.

The signal yields (N_S) are extracted using extended unbinned maximum-likelihood fits to two-dimensional $(\Delta E, M_{bc})$ distributions. An extended likelihood function is:

$$L(N_S, N_{B_j}) = \frac{e^{-(N_S + \sum_j N_{B_j})}}{N!} \prod_{i=1}^N \left[N_S P_S(\Delta E_i, M_{bc_i}) + \sum_j N_{B_j} P_{B_j}(\Delta E_i, M_{bc_i}) \right] \quad (2)$$

where N is the total number of events, i is an index running over the events and P_S and P_{B_j} are the PDFs for signal and background, respectively, and the index j runs over all background sources. The signal yield N_S and background contents N_{B_j} are determined by maximizing the $L(N_S, N_{B_j})$ function, where the variable N_{B_j} defines a j -dimensional submanifold of all different backgrounds.

To take into account the efficiency differences in two data sets, N_S is calculated as:

$$N_S = \epsilon_1 N_{B\bar{B}_1} \mathcal{B} + \epsilon_2 N_{B\bar{B}_2} \mathcal{B}, \quad (3)$$

where \mathcal{B} is a branching fraction, and the ϵ_i and $N_{B\bar{B}_i}$ are the efficiency and the number of $B\bar{B}$ pairs for Set I and Set II. We assume that the numbers of B^+B^- and $B^0\bar{B}^0$ pairs are equal.

For charged B decays, we divide the data into two samples for positive and negative charges and extract the charge asymmetry A_{CP} in addition to the branching fraction \mathcal{B} , using the formula:

$$N_{\pm} = 0.5 (1 \mp A_{CP}) N_S, \quad (4)$$

with N_+ (N_-) the number of positively (negatively) charged kaons or pions and N_S the number of signal events.

The PDF shapes for each contribution are determined by MC studies. We assume the signal shapes for ΔE and M_{bc} to be independent and model the signal using a Gaussian with an exponential tail (Crystal Ball line) [28] plus a Gaussian for ΔE and a Gaussian with an exponential tail for M_{bc} . The shape parameters are fixed from the signal MC sample, except for the means and widths of both ΔE and M_{bc} distributions, which are determined in the fit of $B \rightarrow \eta' K$ for decays with K^+ or K_S^0 in the final state for each data set (Set I and Set II) independently. For $B^+ \rightarrow \eta' \pi^+$ we use the parameters obtained from the fit to the charged kaon mode.

We consider up to four types of backgrounds separately in the fit: continuum, $b \rightarrow c$, two types of charmless decays mentioned below. The ΔE and M_{bc} distributions for continuum backgrounds are found to be largely uncorrelated and are thus modeled with two independent one-dimensional functions. For ΔE we assign a first or second order polynomial and the Argus function [29] is used to model the M_{bc} distribution. Charmless B decays and $b \rightarrow c$ backgrounds are modeled with 2-dimensional smoothed histograms. The contributions from charmless B decays are modeled with two smoothed histograms, one for one decay that makes a large contribution to the background, and one for all other charmless decays. For

$B^+ \rightarrow \eta' K^+$, the dominant decay decay mode that is modeled separately is $B \rightarrow \eta' K^*$; for $B^0 \rightarrow \eta' K_S^0$ it is $B \rightarrow \rho^0 K_S^0$; and for $B^+ \rightarrow \eta' \pi^+$ it is the $B^+ \rightarrow \eta' K^+$ feeddown. The feeddown in $B^+ \rightarrow \eta' \pi^+$ is modeled with the same PDFs as used for the signal, shifted in ΔE and with an additional correction factor for the change in the width in ΔE .

The number of signal and background events are free parameters in the maximum likelihood fit. The signal mean and width shape parameters for kaonic decays and the continuum shape parameters are also free in all fits. For $\eta' \rightarrow \eta \pi^+ \pi^-$ modes our background MC studies show that no contributions from $b \rightarrow c$ decays are expected. For $B \rightarrow \eta' K$ charmless backgrounds are also not expected. For $B^+ \rightarrow \eta' \pi^+$ there is a small contribution from charmless B decays in addition to the $B^+ \rightarrow \eta' K^+$ feeddown. For $\eta' \rightarrow \rho^0 \gamma$ modes, we float the number of events for $b \rightarrow c$ and two charmless B contributions. Other parameters are fixed to values determined from MC or sideband data studies. For the combined results, we use a simultaneous fit with the branching fraction and the charge asymmetry as common parameters for $\eta' \rightarrow \eta \pi^+ \pi^-$ and $\eta' \rightarrow \rho^0 \gamma$. The projection plots of the fits are shown in Fig. 2-4. The reconstruction efficiencies for each decay and results of the fits are displayed in Table I. The upper part of the table displays fit results for individual fits for the two subdecay modes $\eta' \rightarrow \eta \pi^+ \pi^-$ and $\eta' \rightarrow \rho^0 \gamma$. In addition, we list the charge asymmetry of the continuum background obtained from the fits. Since continuum background is thought to be distributed equally for both charges, any significant observed asymmetry would indicate a bias and is therefore included in the systematic error (see below).

We find the significance of $B^+ \rightarrow \eta' \pi^+$ yield is 3.0, which is calculated as $\sigma = \sqrt{2 \ln(L_{\max}/L_0)}$, where L_{\max} and L_0 denote the maximum likelihood value and the likelihood value at zero branching fraction, respectively. The systematic error (mentioned below) is included in the significance calculation by subtracting the systematic error from the obtained branching fraction and recalculating the significance.

The reconstruction efficiencies are determined from signal MC samples before including subdecay branching fractions and are around 16-25% for decays with $\eta' \rightarrow \eta \pi^+ \pi^-$ and 9-12% for $\eta' \rightarrow \rho^0 \gamma$ before considering subdecay branching fractions. The efficiencies are calculated separately for both Set I and Set II. The efficiency for Set II is typically about 0.5% larger than for Set I. Correction factors due to differences between data and MC are included for the charged track identification, photon, π^0 and η reconstruction, resulting in a correction factor of ~ 0.9 . The corrections were determined from detailed studies that are discussed in the section on the systematic error below.

We calculate a goodness of fit (*gof*) based on binned projections of the 2-dim. fit into ΔE . We define:

$$gof = \chi^2 / dof, \quad (5)$$

with $\chi^2 = \sum_{i=1}^N \frac{(n_i - \nu_i)^2}{\nu_i}$ the sum over all bins of the projections with n_i and ν_i the number of expected and observed events in each bin, and *dof* the degrees of freedom. Since we use an unbinned simultaneous fit in ΔE and M_{bc} the projected *gof* value is not a rigorous estimator but can still be used to qualitatively evaluate how well we fit the data.

Systematic errors are estimated with various high statistics data samples. The sources and their contributions are listed in Table II. The dominant sources of background are the uncertainties of the reconstruction efficiency of charged tracks, the uncertainties in the reconstruction efficiencies for η mesons and photons and the uncertainty of the PDFs shape and other parameters, which are estimated by varying each parameter of the PDFs by the 1σ uncertainty in its nominal value. The changes in the yield are added in quadrature.

TABLE I: Signal efficiencies with (ϵ_{tot}) and without (ϵ) subdecay branching fractions included and averaged for Set I and Set II for $\eta' \rightarrow \eta\pi^+\pi^-$ and $\eta' \rightarrow \rho^0\gamma$, branching ratios \mathcal{B} , asymmetry A_{CP} for signal and background and goodness of fit (gof). The errors in ϵ are statistical uncertainties in the MC while those in ϵ_{tot} include errors of secondary branching fractions. For others, the first errors are statistical and the second (if given) are systematic errors.

	$B^+ \rightarrow \eta' K^+$	$B^0 \rightarrow \eta' K^0$	$B^+ \rightarrow \eta' \pi^+$
$\epsilon(\eta' \rightarrow \eta\pi^+\pi^-)$ [%]	25.23 ± 0.11	19.9 ± 0.16	16.3 ± 0.10
$\epsilon_{\text{tot}}(\eta' \rightarrow \eta\pi^+\pi^-)$ [%]	4.41 ± 0.14	1.20 ± 0.04	2.85 ± 0.10
yield ($\eta' \rightarrow \eta\pi^+\pi^-$)	1140.7 ± 43.9	243.2 ± 21.9	17.4 ± 7.0
$\mathcal{B}(\eta' \rightarrow \eta\pi^+\pi^-)$ [10^{-6}]	67.1 ± 2.6	$52.5^{+4.8}_{-4.7}$	$1.58^{+0.78}_{-0.70}$
$A_{CP}(\eta' \rightarrow \eta\pi^+\pi^-)$	-0.003 ± 0.036	—	$0.25^{+0.49}_{-0.47}$
$\epsilon(\eta' \rightarrow \rho^0\gamma)$ [%]	10.06 ± 0.09	11.6 ± 0.19	9.5 ± 0.08
$\epsilon_{\text{tot}}(\eta' \rightarrow \rho^0\gamma)$ [%]	2.97 ± 0.10	1.18 ± 0.04	2.80 ± 01.0
yield ($\eta' \rightarrow \rho^0\gamma$)	823.3 ± 42.9	278.3 ± 24.1	23.9 ± 10.1
$\mathcal{B}(\eta' \rightarrow \rho^0\gamma)$ [10^{-6}]	$71.9^{+3.8}_{-3.7}$	$61.1^{+5.4}_{-5.2}$	2.21 ± 1.28
$A_{CP}(\eta' \rightarrow \rho^0\gamma)$	0.09 ± 0.05	—	$-0.09^{+0.66}_{-0.74}$
yield	1952.2 ± 60.6	519.9 ± 32.3	37.8 ± 14.5
$\mathcal{B}[10^{-6}]$	$68.6 \pm 2.1 \pm 3.6$	$56.6^{+3.6+3.3}_{-3.5-3.2}$	$1.73^{+0.69}_{-0.63} \pm 0.12$
A_{CP}	$0.029 \pm 0.028 \pm 0.02$	—	$0.15^{+0.39+0.02}_{-0.38-0.06}$
$A_{CP}(\text{continuum})$	$-0.013^{+0.008}_{-0.006}$	—	$0.018^{+0.006}_{-0.023}$
gof	1.14	1.51	1.16

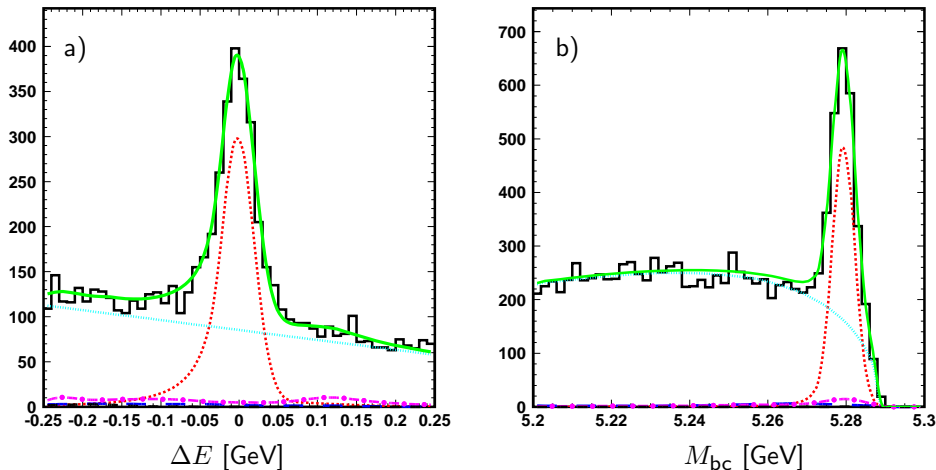


FIG. 2: a) ΔE and b) M_{bc} distributions for $B^+ \rightarrow \eta' K^+$ (for $\eta' \rightarrow \eta\pi^+\pi^-$ and $\eta' \rightarrow \rho^0\gamma$ combined) for the region $M_{bc} > 5.27$ GeV and -0.1 GeV $< \Delta E < 0.06$ GeV, respectively. The histograms represent data, the red small dashed line the signal contribution, the light blue dotted line continuum background, the dark blue large dashed line $b \rightarrow c$ backgrounds and the pink dash-dotted line charmless B contributions. The green solid line is the sum of all contributions to the fit.

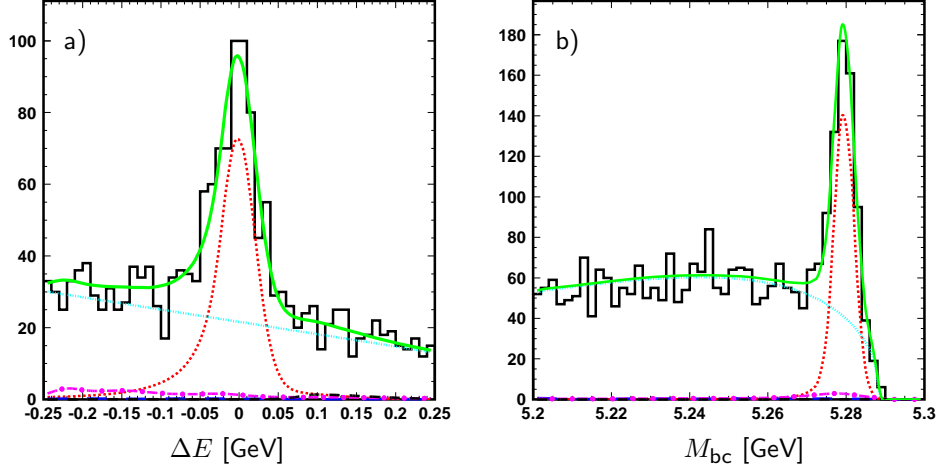


FIG. 3: a) ΔE and b) M_{bc} distributions for $B^0 \rightarrow \eta' K_S^0$ (for $\eta' \rightarrow \eta\pi^+\pi^-$ and $\eta' \rightarrow \rho^0\gamma$ combined) for the region $M_{bc} > 5.27$ GeV and -0.1 GeV $< \Delta E < 0.06$ GeV, respectively. The histograms represent data, the red small dashed line the signal contribution, the light blue dotted line continuum background, the dark blue large dashed line $b \rightarrow c$ backgrounds and the pink dash-dotted line charmless B contributions. The green solid line is the sum of all contributions to the fit.

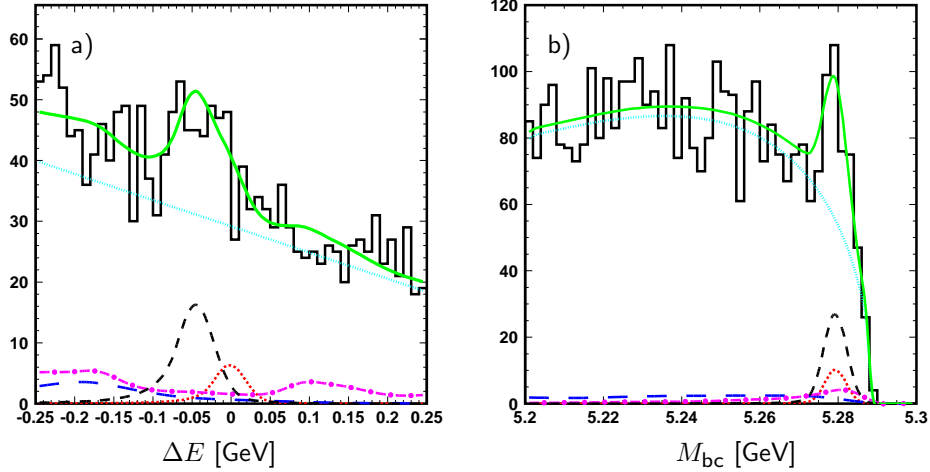


FIG. 4: a) ΔE and b) M_{bc} distributions for $B^+ \rightarrow \eta' \pi^+$ (for $\eta' \rightarrow \eta\pi^+\pi^-$ and $\eta' \rightarrow \rho^0\gamma$ combined) for the region $M_{bc} > 5.27$ GeV and -0.1 GeV $< \Delta E < 0.06$ GeV, respectively. The histograms represent data, the red small dashed line the signal contribution, the light blue dotted line continuum background, the dark blue large dashed line $b \rightarrow c$ backgrounds, the pink dash-dotted line charmless B contributions and the black medium dashed line $B^+ \rightarrow \eta' K^+$ feeddown. The green solid line is the sum of all contributions to the fit.

The normalization of the K feeddown to $B^+ \rightarrow \eta' \pi^+$ is estimated by varying the assumed branching fraction for the feeddown by the $\pm 1\sigma$ uncertainty in the present measurement of $B^+ \rightarrow \eta' K^+$, the error arising from differences in the fake efficiency is included in the systematic error for the PDF parameters. Corrections for ΔE and M_{bc} differences between data and MC for the feeddown shape of $\eta' K$ to $B^+ \rightarrow \eta' \pi^+$ are considered by varying the corrections by one standard deviation and refitting. Systematics arising from the $\mathcal{R}_{\mathcal{L}}$

selection are studied by varying the $\mathcal{R}_{\mathcal{L}}$ selection and by a large $B \rightarrow D\pi$ sample, we conservatively use the larger error. The uncertainty of the subdecay branching fractions is given in the PDG. The number of $B\bar{B}$ mesons produced at Belle is estimated from the number of continuum-subtracted hadronic events. The uncertainty in this value is included in the systematic error. The uncertainty of the particle identification is estimated with $D^{*+} \rightarrow D^0\pi^+$ decays. Other efficiency systematic errors are found to add up to less than 1% and are included with a 1% error. All contributions are added in quadrature and we find the systematic errors for the three decays to lie between 5% and 7%. For the charge asymmetry, efficiency based systematic errors cancel out and therefore we use the high statistics mode $B^+ \rightarrow \eta'K^+$ to calculate systematic errors and use the same absolute numbers for $B \rightarrow \eta'\pi$. The dominant contribution to the A_{CP} systematic error is from the possible difference in the detector response for positive and negative charged particles. We estimate this from the continuum asymmetry to be 0.02. Other contributions from fitting and normalization together result in a systematic error of 0.002. Thus the total systematic error for the A_{CP} measurement is 0.02. For $B^+ \rightarrow \eta'\pi^+$ we assign an additional source of error by adding an asymmetry to the $B^+ \rightarrow \eta'K^+$ feeddown contribution. We find an error of -0.06 , which is added in quadrature to the other errors.

TABLE II: A breakdown of systematic uncertainties in percentage for branching fraction measurements. Systematic errors from tracking, $\epsilon_{\gamma,\pi^0,\eta}$, the combined systematics from these three particles, particle ID, ϵ , the systematics from efficiency calculations, $\mathcal{R}_{\mathcal{L}}$ selection, PDF, from varying the fit parameters by one σ , $\Delta E/M_{bc}$ corrections, which are varied by $\pm 1\sigma$, the $B^+ \rightarrow \eta'K^+$ feeddown to $B^+ \rightarrow \eta'\pi^+$, \mathcal{B}_s , the subdecay branching fraction errors and $N_{B\bar{B}}$, the uncertainty of the number of $B\bar{B}$, are listed.

Source	$\Delta\mathcal{B}/\mathcal{B}$ [%]		
	$B^+ \rightarrow \eta'K^+$	$B^+ \rightarrow \eta'\pi^+$	$B^0 \rightarrow \eta'K_S^0$
tracking	3	3	4
$\epsilon_{\gamma,\pi^0,\eta}$	3	3	3
part. ID	0.7	0.9	0.6
ϵ	1	1	1
$\mathcal{R}_{\mathcal{L}}$	2	+1.9 -2.7	2
PDF	+0.5 -0.7	+2.6 -2.0	+1.2 -1.3
$\Delta E/M_{bc}$	—	+2.1 -1.9	—
$\eta'K^+$ feeddown	—	+3.5 -2.9	—
\mathcal{B}_s	1.5	1.5	1.5
$N_{B\bar{B}}$	1	1	1
Total	5.2	+7.1 -6.8	5.9

In summary, we report improved measurements with 35 times more statistics of the charged and neutral $B \rightarrow \eta'K$ decay. We find 3σ evidence for $B^+ \rightarrow \eta'\pi^+$ and report the charge asymmetry for the decay modes $B^+ \rightarrow \eta'K^+$ and $B^+ \rightarrow \eta'\pi^+$. The central values of our branching fraction measurements are below current PDG values, but are consistent within statistical errors.

We thank the KEKB group for the excellent operation of the accelerator, the KEK cryogenics group for the efficient operation of the solenoid, and the KEK computer group and the National Institute of Informatics for valuable computing and Super-SINET network support. We acknowledge support from the Ministry of Education, Culture, Sports, Science, and Technology of Japan and the Japan Society for the Promotion of Science; the Australian Research Council and the Australian Department of Education, Science and Training; the National Science Foundation of China under contract No. 10175071; the Department of Science and Technology of India; the BK21 program of the Ministry of Education of Korea and the CHEP SRC program of the Korea Science and Engineering Foundation; the Polish State Committee for Scientific Research under contract No. 2P03B 01324; the Ministry of Science and Technology of the Russian Federation; the Ministry of Higher Education, Science and Technology of the Republic of Slovenia; the Swiss National Science Foundation; the National Science Council and the Ministry of Education of Taiwan; and the U.S. Department of Energy.

-
- [1] Y. Grossman and M. P. Worah, *Phys. Lett.* **B395** (1997) 241, hep-ph/9612269,
 - [2] D. Atwood and A. Soni, *Phys. Lett.* **B405** (1997) 150, hep-ph/9704357.
 - [3] E. Kou, *Phys. Rev.*, **D63** (2001) 054027, hep-ph/9908214.
 - [4] Throughout this paper, the inclusion of the charge conjugate mode decay is implied unless otherwise stated.
 - [5] S. J. Richichi *et al.* (CLEO Collaboration), *Phys. Rev. Lett.* **85** (2000) 520, hep-ex/9912059.
 - [6] K. Abe *et al.* (Belle Collaboration), *Phys. Lett.* **B517** (2001) 309, hep-ex/0108010.
 - [7] B. Aubert *et al.* (BABAR Collaboration), *Phys. Rev. Lett.* **91** (2003) 161801, hep-ex/0303046.
 - [8] A. Ali, G. Kramer, and C.-D. Lu, *Phys. Rev.* **D58** (1998) 094009, hep-ph/9804363.
 - [9] Y.-H. Chen, H.-Y. Cheng, B. Tseng, and K.-C. Yang, *Phys. Rev.* **D60** (1999) 094014, hep-ph/9903453.
 - [10] E. Kou and A. I. Sanda, *Phys. Lett.* **B525** (2002) 240, hep-ph/0106159.
 - [11] C.-W. Chiang and J. L. Rosner, *Phys. Rev.* **D65** (2002) 074035, hep-ph/0112285.
 - [12] W.-S. Hou and B. Tseng, *Phys. Rev. Lett.* **80** (1998) 434, hep-ph/9705304.
 - [13] F. Yuan and K.-T. Chao, *Phys. Rev.* **D56** (1997) 2495, hep-ph/9706294.
 - [14] D.-s. Du, C. S. Kim, and Y.-d. Yang, *Phys. Lett.* **B426** (1998) 133, hep-ph/9711428.
 - [15] M. R. Ahmady, E. Kou, and A. Sugamoto, *Phys. Rev.* **D58** (1998) 014015, hep-ph/9710509.
 - [16] Z.-j. Xiao, W.-j. Li, L.-b. Guo, and G.-r. Lu, *Mod. Phys. Lett.* **A16** (2001) 441, hep-ph/0103152.
 - [17] B. Dutta, C. S. Kim, and S. Oh, *Nucl. Phys. Proc. Suppl.* **111** (2002) 273, hep-ph/0207171.
 - [18] S. Khalil and E. Kou, *Phys. Rev. Lett.* **91** (2003) 241602, hep-ph/0303214.
 - [19] M.-A. Dariescu and C. Dariescu, *Eur. Phys. J.* **C36** (2004) 215, hep-ph/0404148.
 - [20] G. Kramer, and W. F. Palmer, and H. Simma, *Nucl. Phys.* **B428** (1994), 77, hep-ph/9402227,
 - [21] S. Kurokawa and E. Kikutani, *Nucl. Instr. and Meth.* **A499** (2003) 1, and other papers included in this volume.
 - [22] A. Abashian *et al.* (Belle Collab.), *Nucl. Instr. and Meth.* **A479**, 117 (2002).
 - [23] Y. Ushiroda (Belle SVD2 Group), *Nucl. Instr. and Meth.* **A511** 6 (2003).
 - [24] S. Eidelman *et al.* (Particle Data Group), *Phys. Lett.* **B592** (2004) 1.
 - [25] The Fox-Wolfram moments were introduced in G. C. Fox and S. Wolfram, *Phys. Rev. Lett.* **41**,

- 1581 (1978). The Fisher discriminant used by Belle, based on modified Fox-Wolfram moments (SFW), is described in K. Abe *et al.* (Belle Collab.), *Phys. Rev. Lett.* **87**, 101801 (2001) and K. Abe *et al.* (Belle Collab.), *Phys. Lett.* **B 511**, 151 (2001).
- [26] R. A. Fisher, *Annals of Eugenics* **7** (1936) 179.
- [27] H. Kakuno *et al.*, *Nucl. Instr. and Meth.* **A533** 516 (2004).
- [28] J.E.Gaiser *et al.* (Crystal Ball Collaboration) *Phys. Rev.* **D34**, 711 (1986).
- [29] H. Albrecht *et al.* (ARGUS Collaboration), *Phys. Lett.* **B241** (1990) 278.